

Al compositional inhomogeneity of AlGaN epilayer with a high Al composition grown by metal–organic chemical vapour deposition

This article has been downloaded from IOPscience. Please scroll down to see the full text article.

2007 J. Phys.: Condens. Matter 19 176005

(<http://iopscience.iop.org/0953-8984/19/17/176005>)

View [the table of contents for this issue](#), or go to the [journal homepage](#) for more

Download details:

IP Address: 129.252.86.83

The article was downloaded on 28/05/2010 at 17:53

Please note that [terms and conditions apply](#).

Al compositional inhomogeneity of AlGa_N epilayer with a high Al composition grown by metal–organic chemical vapour deposition

X L Wang^{1,3}, D G Zhao¹, D S Jiang¹, H Yang¹, J W Liang¹, U Jahn² and K Ploog²

¹ State Key Laboratory on Integrated Optoelectronics, Institute of Semiconductors, Chinese Academy of Sciences, PO Box 912, Beijing 100083, People's Republic of China

² Paul-Drude-Institut für Festkörperelektronik, Hausvogteiplatz 5–7, 10117 Berlin, Germany

E-mail: WXL@mail.semi.ac.cn

Received 17 January 2007, in final form 26 February 2007

Published 10 April 2007

Online at stacks.iop.org/JPhysCM/19/176005

Abstract

The Al compositional distribution of AlGa_N is investigated by cathodoluminescence (CL). Monochromatic CL images and CL spectra reveal a lateral Al compositional inhomogeneity, which corresponds to surface hexagonal patterns. Cross-sectional CL images show a relatively uniform Al compositional distribution in the growth direction, indicating columnar growth mode of AlGa_N films. In addition, a thin AlGa_N layer with lower Al composition is grown on top of the buffer AlN layer near the bottom of the AlGa_N epilayer because of the larger lateral mobility of Ga adatoms on the growth surface and their accumulation at the grain boundaries.

1. Introduction

AlGa_N has been developed for applications in ultraviolet (UV) light emitters, UV photodetectors, white light emitters [1, 2] and high-power electronics [3] because of its low natural background in the solar-blind region (290–240 nm). Generally, the AlGa_N materials used in the fabrication of those devices are grown by low-pressure metal–organic chemical vapour deposition on double-side-polished (0001) sapphire substrates. There is a well-known difficulty in growing such materials due to the low surface mobility of Al atoms. The Al composition has an inhomogeneous distribution and the crystal quality is degraded with increasing aluminium content in the preparation of high Al-content AlGa_N. One phenomenon related to the Al composition inhomogeneity is the compositional pulling effect, where the compositional inhomogeneity caused by the large strain between AlGa_N and GaN occurs in the growth direction. The other is lateral phase separation. Several groups have investigated

³ Author to whom any correspondence should be addressed.

these phenomena [4–7]; however, there are few reports on the detailed spatial distribution of the Al composition, especially in AlGa_N epilayers with high Al content.

In this paper, we report an investigation of the Al compositional distribution of AlGa_N epilayers with high Al content and we analyse the correlation between the growth mechanism and the compositional inhomogeneity. By using cathodoluminescence (CL) spectra and CL micro-images taken at different photon energies, a difference in the distributions of Al composition in the lateral and vertical directions was observed.

2. Experiments

AlGa_N samples were grown by low-pressure metal–organic chemical vapour deposition (MOCVD) on (0001) sapphire substrates. Trimethylgallium, trimethylaluminium, and ammonia were used as Ga, Al, and N sources, respectively. Prior to growth, the surface of the substrate was cleaned in hydrogen atmosphere and then the surface was nitrided with ammonia at high temperature. During the growth of the AlGa_N epilayer, a small amount of trimethylindium was added to the growth ambient to enhance the surface migration of absorbed Al species [8]. AlN/AlGa_N superlattices (SLs) were inserted as a buffer layer to play the role of a dislocation filter to suppress the material mosaicity and decrease the threading dislocation density [9]. Then a thin high-temperature (HT) AlN layer was grown on the superlattice. Finally, a 1.5 μm-thick AlGa_N epilayer was deposited on the complex buffer, with hydrogen employed as the carrier gas. A growth pressure of 100 Torr and an approximate temperature of 1100 °C were used during growth. The Al composition of the AlGa_N epilayers was set to nearly 0.53. X-ray diffraction (XRD) measurement was performed using a Rigaku SLX-1A x-ray diffractometer equipped with a Si(220) analyser. Low-temperature CL investigations were performed with a scanning electron microscope (SEM) equipped with an Oxford mono CL2 and He-cooling stage operating at 6 K. A grating monochromator and a cooled charge-coupled device array were used to disperse and detect the CL signal, respectively.

3. Result and discussion

Typical full widths at half maximum (FWHM) of the AlGa_N(0002) and (10–12) x-ray diffraction rocking curves are 600 and 960 arc sec, respectively. The Al composition is determined to be approximately 0.5 in the AlGa_N epilayer, according to the peak position of XRD. Figure 1(a) shows the (0002) rocking curve of the sample. A shoulder appears on the right side of the AlGa_N XRD peak, indicating that there may be compositional inhomogeneity of Al in the AlGa_N epilayer.

In order to clarify the phenomenon of compositional inhomogeneity of Al atoms, a CL study was performed. The CL spectra were recorded with an electron beam focused on the surface of the AlGa_N epilayer. An acceleration voltage of 5 kV was used, giving a penetration depth of approximately 200 nm [10]. Assuming a very short diffusion length (<200 nm in AlGa_N) of the generated carriers in the AlGa_N film, the major part of the observed luminescence originated from the top 200 nm of the film. Figure 1(b) is the CL spectrum recorded at 6 K taken from a large surface area of the sample. The CL spectrum has a strong peak at the high-energy side, which is assigned to the near-band-edge (NBE) emission with a shoulder at the lower-energy side. We can attribute the shoulder to the inhomogeneous distribution of the aluminium. Monochromatic CL images taken at photon energies of 4.42 and 4.12 eV of the same surface area as figure 2(a) are shown in figures 2(b) and (c), respectively, which correspond to the NBE emission peak and the shoulder in the CL spectrum in figure 1(b), respectively. The energy values are marked by arrows in figure 1(b). Figure 2(a) is the SEM

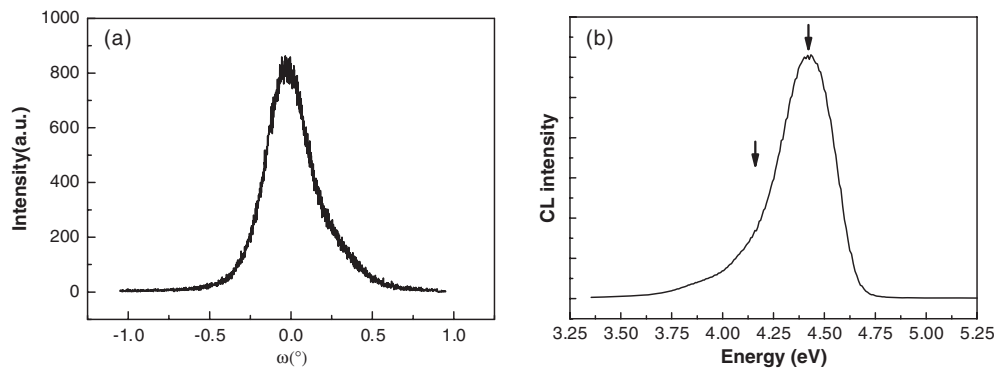


Figure 1. (a) The (0002) double-axis x-ray diffraction patterns and (b) CL spectrum ($T = 6$ K, averaged over $100 \mu\text{m} \times 100 \mu\text{m}$) of an AlGaIn epilayer.

image of the sample, and this shows that the sample has a well-ordered surface and exhibits the distinct characteristics of spiral-growth-formed truncated hexagonal pyramids with large and regular terraces. The pyramids are about $1 \mu\text{m}$ in diameter. Figure 2(b) shows some domain-like structures. The bright domains correspond to hexagonal patterns in the SEM image of figure 2(a). The size of the domains shown in figure 2(b) is larger than that of the hexagonal pyramids shown in figure 2(a). The boundaries of the bright domains are narrower than those in the SEM image. Such a correspondence may be related to the growth mode of the AlGaIn epilayer and may be considered a result of columnar growth (as described below), besides the cause that the CL image is formed from light collected to a depth of 200 nm into the sample while the secondary electrons that contribute to the SEM image originate from a depth of the order of a few nanometres. We were surprised to find that the boundaries of the domains are dark in figure 2(b), opposite to those in figure 2(c). In addition, the bright domains in figure 2(b) are just the dark ones in figure 2(c). Therefore, the CL images taken at two different energies are entirely complementary. Moreover, many dark spots in both images are located at the same position. Those dark spots are believed to be associated with the presence of defects, which act as non-radiative recombination centres [11].

More details about the luminescence variations can be obtained through recording a series of CL spectra at points along a line on the AlGaIn surface through a line scan of CL spectra, as shown in figure 3(b). The line scan measurements were performed from the left-hand side towards the right-hand side, crossing two islands along the line, as shown in figure 3(a), with a constant step length. Each step covers a lateral distance of 200 nm. There are two distinct CL peaks located at 4.52 and 4.43 eV, which come mainly from the islands and the gaps between them, respectively. They are the near-band-edge emissions of AlGaIn alloy film, and they suggest that the AlN mole fraction is lower in the gaps than in the islands. Moreover, the intensity of luminescence at the middle of domains is stronger than that at the boundaries of domains. This may be due to the high defect density at the boundary regions.

Many groups found that a compositional inhomogeneity exists in the longitudinal direction of the AlGaIn films. We have examined the cross-sectional CL images taken at different photon energies to analyse the Al compositional distribution in the vertical direction. During cross-sectional measurements, the cleaved sample surface was not set horizontal but tilted at a small angle in order to partly show the sample surface area in the obtained SEM and CL images. In this way it was possible to check the relation between surface morphology and the vertical distribution of structural properties. Figure 4(a) is a cross-sectional SEM image of the $1.5 \mu\text{m}$ -

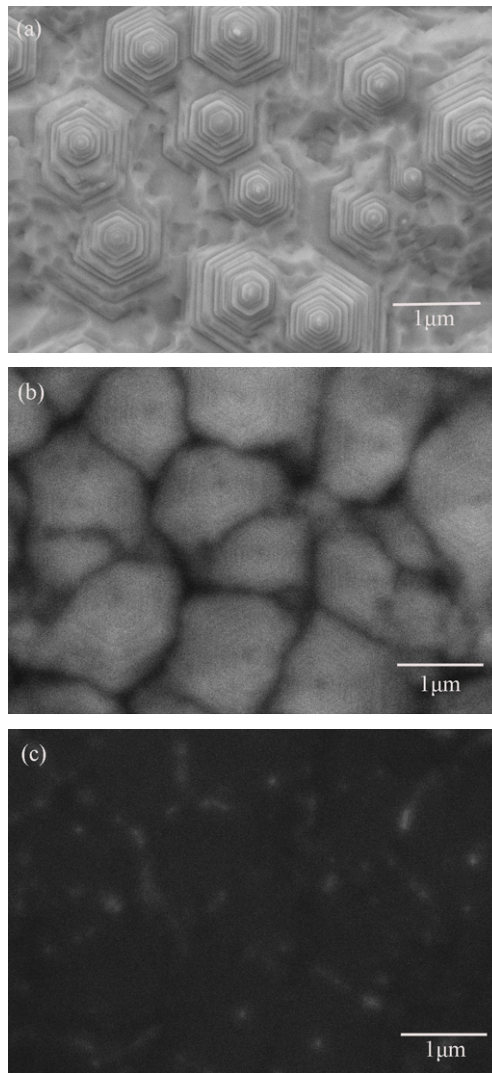


Figure 2. SEM image and CL images taken at different energies of AlGaIn epilayer over the same area: (a) the SEM image; (b) and (c) CL images at 4.42 and 4.12 eV, respectively.

thick AlGaIn epilayer grown on sapphire. To determine the exact origin of the luminescence, two CL images are taken at 4.42 and 3.75 eV, as shown in figures 4(b) and (c), respectively. For the selective-energy CL image at 4.42 eV, the bright emission extends from the front surface downwards and diminishes near the complex buffer layer, forming a column-like pattern. It is noted that when the photon energy for CL imaging is red-shifted to, for example, near 3.75 eV, the emission from the front surface becomes much weaker, and the bright emission occurs at the top of the HT AlN near the AlGaIn epilayer. This is attributed to the lower Al composition in this region of the AlGaIn layer. Figure 4(b) shows that the bright emission extends almost to the entire AlGaIn epilayer thickness. This result provides direct evidence that the compositional inhomogeneity does not apparently exist in the growth direction of an AlGaIn film grown on complex buffer-coated (0001) sapphire. It is confirmed that the shoulder

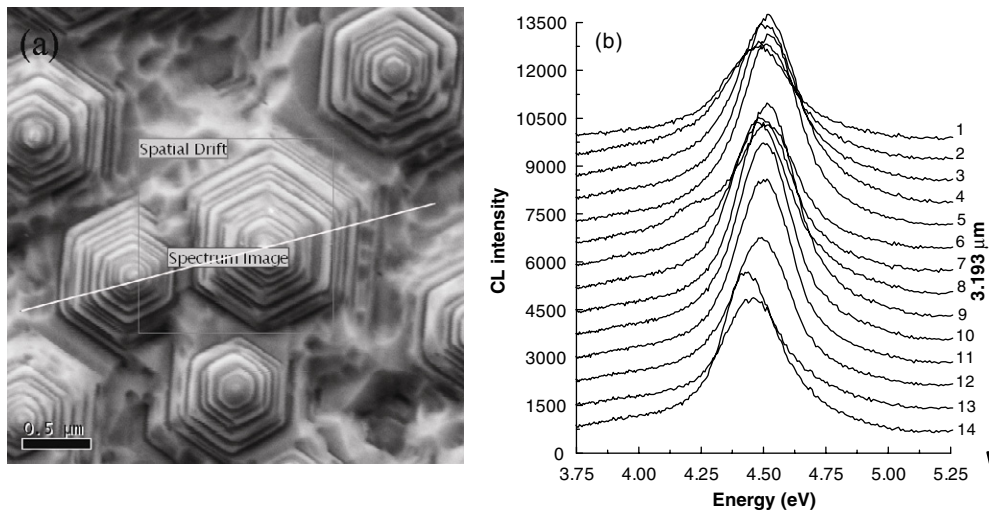


Figure 3. (a) Monochromatic CL image of domains in the sample; (b) the lateral line scan CL spectra across the domains along the line shown in figure 3(a). Each step covers a lateral distance of 200 nm.

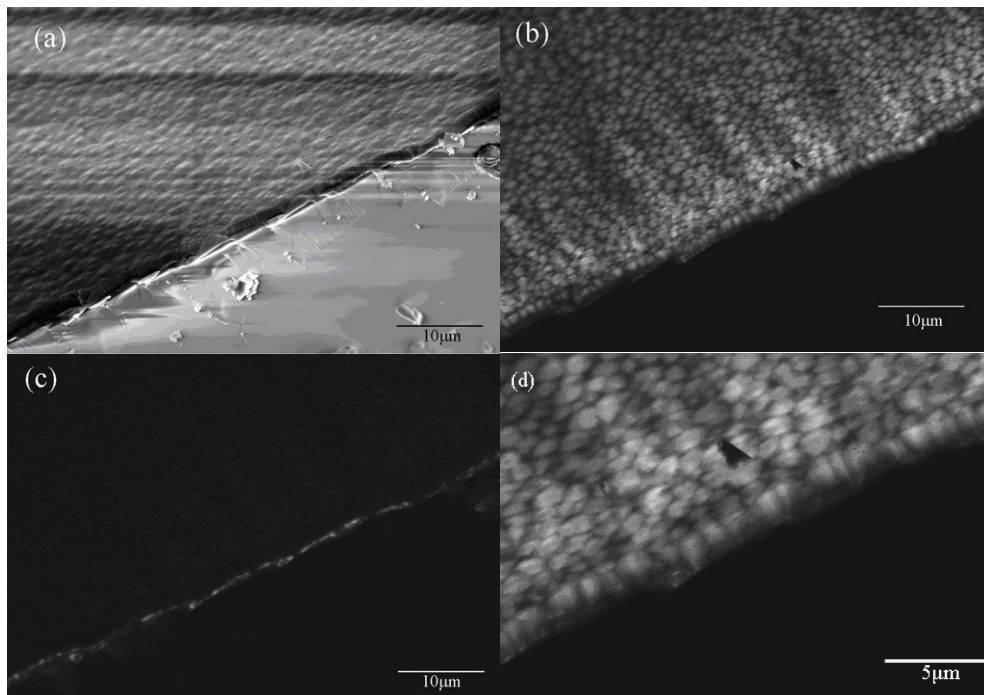


Figure 4. (a) Cross-sectional scanning electron microscopy profile of AlGaIn epilayer on sapphire; (b) and (c) are the CL images taken at 4.42, 3.75 eV, respectively; (d) a magnified region of (b).

in the large-surface-area CL spectrum shown in figure 1(b) comes only from the lateral Al compositional inhomogeneity.

In order to check the origin of luminescence with energy at 3.75 eV in the thin HT AlGaIn region, it is necessary to analyse the growth mechanism of the AlGaIn sample. Due to the thick complex buffer and lower lateral mobility of Al adatoms on the growth surface, the surface of the HT buffer AlN layer is very coarse (as speculated by the traces of *in situ* optical reflectivity of the sample, not shown here). The diameter and height of the surface islands are very large. Because Ga adatoms have a larger lateral mobility than Al adatoms, Ga adatoms reach the boundary of the islands more quickly than Al atoms. When AlGaIn is grown on the HT buffer AlN layer, the boundaries of the islands are filled with a large quantity of Ga adatoms with a lower Al composition. Therefore, a thin AlGaIn layer with lower Al composition is formed, giving a luminescence peak at 3.75 eV, as shown in figure 3. The islands and boundaries grow continuously in the vertical direction during the AlGaIn epilayer growth, with the boundary regions filled with AlGaIn of lower Al composition. This is the reason for the columnar growth of the AlGaIn shown in figure 4(d). In figure 4(d) it is also possible to see that bright domains on the surface are connected with the bright columns, indicating the correlation between surface morphology and the columnar growth mechanism. The truncated hexagonal pyramids with large and regular terraces show a feature of spiral growth. Because of the low lateral migration of Al adatoms on the growing surface, the size of hexagonal pyramids becomes smaller when the AlGaIn growth continues, leading to a larger size of CL domains than the pyramid patterns emerging in the corresponding SEM image.

4. Conclusions

In conclusion, we have reported our investigation of the Al compositional inhomogeneity of AlGaIn epilayers via CL spectra and monochromatic images. Plane and cross-sectional CL images show that an AlGaIn epilayer has a relatively homogenous distribution of Al composition in the vertical growth direction, while it has a remarkable inhomogeneity in the lateral direction, confirming a columnar growth mechanism of AlGaIn epitaxy.

References

- [1] Lambert D J H, Wong M M, Chowdhury U, Collins C, Li T, Kwon H K, Shelton B S, Zhu T G, Campbell J C and Dupuis R D 2000 *Appl. Phys. Lett.* **77** 1900
- [2] Chitnis A, Zhang J P, Adivarahan V, Shatalov M, Wu S, Pachipulusu R, Mandavilli V and Asif Khan M 2003 *Appl. Phys. Lett.* **82** 2565
- [3] Chumbes E M, Schremer A T, Smart J A, Wang Y, MacDonald N C, Hogue D, Komiak J J, Lichwalla S J, Leoni R E and Shealy J R 2001 *IEEE Trans. Electron.* **48** 420
- [4] Sun Q, Huang Y, Wang H, Chen J, Jin R Q, Zhang S M, Yang H, Jiang D S, Jahn U and Ploog K H 2005 *Appl. Phys. Lett.* **87** 121914
- [5] Hiramatsu K, Kawaguchi Y, Shimizu M, Sawaki N, Zheleva T, Davis R F, Tsuda H, Taki W, Kuwano N and Oki K 1997 *MRS Internet J. Nitride Semicond. Res.* **2** 6
- [6] Tsai Y-L, Wang C-L, Lin P-H, Liao W-T and Gong J-R 2003 *Appl. Phys. Lett.* **82** 31
- [7] Lin H Y, Chen Y F, Lin T Y, Shih C F, Liu K S and Chen N C 2006 *J. Cryst. Growth* **290** 22
- [8] Keller S, Heikman S, Ben-yaacov I, Shen L, DenBaars S P and Mishra U K 2001 *Phys. Status Solidi a* **188** 775
- [9] Wang H-M, Zhang J-P, Chen C-Q, Fareed Q, Yang J-W and Asif Khan M 2002 *Appl. Phys. Lett.* **81** 604
- [10] Goldstein J I, Newbury D E, Echlin P, Joy D C, Roming A D, Lyman C E, Fiori C and Lifshin E 1992 *Scanning Electron Microscopy and X-Ray Microanalysis* (New York: Plenum)
- [11] Sugahara T, Sato H, Hao M, Naoi Y, Kurai S, Tottori S, Yamashita K, Nishino K, Romano L T and Sakai S 1998 *Japan. J. Appl. Phys.* **37** L398